Electrochemical and Surface-Enhanced Raman Spectroscopic Studies on the Adsorption and Electrooxidation of C_1 Molecules on a Roughened Rh Electrode

Xu-Feng Lin,[†] Bin Ren,*[,†] and Zhong-Qun Tian[‡]
Department of Chemistry, State Key Laboratory for Physical Chemistry of Solid Surfaces, Xiamen University, Xiamen 361005, China
Received: May 23, 2003; In Final Form: October 29, 2003

By using the previously developed roughening method for producing SERS-active Rh electrode, and assisted by the highly sensitive confocal microprobe Raman system, we carried out a detailed SERS study on the dissociation and electrooxidation of C_1 molecules on a Rh surface. The SERS spectra obtained in a wide frequency region provide not only the vibrations reflecting the internal bonding of CO (at ca. 2000 cm^{-1}) but also the bonding between CO or O with Rh (at ca. 450 cm^{-1}). A complementary electrochemical study was also performed on the roughened Rh surface in order to correlate the electrochemical and vibrational information. Both electrochemical and SERS studies show that Rh has no discernible activity toward the electrooxidation or dissociation of methanol in acidic solutions. Rh becomes active and its activity increases with the decrease of the solution acidity. For HCHO and HCOOH, the electrooxidation activity of Rh increases with increasing pH. On the basis of the result of the model CO system, discussion on the dissociation or electrooxidation mechanisms was presented for C_1 molecules on Rh.

Introduction

The chemistry dealing with molecules containing one carbon atom and relevant small molecules, so-called C_1 chemistry, is of great significance for environmental protection. The electrooxidation of C_1 molecules has been widely investigated in the past 30 years mainly because of their significant role in fuel cells. Pt-group metals play a key role in this field because of their high catalytic performance. To study the electrooxidation processes, a number of in-situ and ex-situ methods have been employed, such as electrochemical techniques,[1−6] infrared reflection−adsorption spectroscopy,[7−13] surface-enhanced Raman spectroscopy (SERS),[14−16] infrared−visible sum frequency generation,[17−19] electron energy loss spectroscopy,[20,21] low-energy electron diffraction,[22] differential electrochemical mass spectroscopy,[23−25] and NMR.[26] Despite these efforts, the mechanisms of the electrooxidation of the C_1 molecules on Pt-group metals have not been well understood, mainly because the oxidation of these molecules usually occurs via several one- or multielectron-transfer steps.

Among vibrational spectroscopies that are available for studying adsorbates on surfaces at the molecular level, SERS is more and more recognized as a versatile probe for investigating both solid/liquid and solid/gas interfaces.[27−34] SERS is particularly valuable for the study of aqueous electrochemical interfaces, because of negligible absorbance of the visible light by water. Additional advantage of Raman spectroscopy is its wide frequency range (ca. 0−4000 cm^{-1}). This includes a particularly interesting region below 800 cm^{-1}, where the vibrational features of the metal−adsorbate bonds normally appear. However, the application of SERS has been seen to be restricted to coinage-metal substrates because only coinage-metal substrates can support giant surface enhancement for Raman scattering of surface species. This view changed in the late 1990s. SERS has been observed also for adsorbates on transition metals as a result of two key developments: the improvement of the detection sensitivities and the spatial resolution when employing a confocal Raman microscopes, and the tremendous effort in a specific preparation of the transition-metal substrates. Weaver's group has focused on the preparation of ultrathin Pt-group metal films coated over SERS-active gold electrodes by electrodeposition.[35] Although they have made great improvement on their thin-film strategy,[36−38] there still remain some problems such as the stability and homogeneity of these films and their SERS activities in a wide potential range (i.e., reversibility). A still-open question is how the noble-metal substrates affect the physiochemical properties of the transition-metal overlayers. An alternative way to create SERS at transition-metal surfaces is to recur to procedures used to make the noble-metal SERS active, i.e., the surface roughening of a pure massive metal substrate without the complication from the SERS from the underlying substrate. Our group has created and developed several specific roughening methods suitable to make massive transition metals SERS-active.[34,39−42] In fact, the SERS signals of a variety of adsorbates at these metals have been obtained.[34,39,42] For Rh, a controlled square-wave current roughening method has been developed,[43,44]which produces a SERS-active Rh substrate with high stability, reversibility, and reusability after electrochemical cleaning without re-roughening. The most important is that the electrochemical properties of the surface is very similar to that of the smooth Rh surface, which ensures the SERS study on this surface is also in representative for a smooth surface.[44] In this paper, we report a systematic study on the adsorptions and reactions of various C_1 molecules on a Rh electrode in solutions with different acidity.

Experimental Section

The roughening procedure for creating a SERS-active Rh electrode has been reported elsewhere,[43,44] which produces a very stable and reversible Rh substrate that enables the results from different systems to be highly comparable. A large

* Author to whom correspondence should be addressed. Tel: 86-592-2181906, Fax: 86-592-2085349. E-mail: bren@jingxian.xmu.edu.cn.
[†] Department of Chemistry.
[‡] State Key Laboratory for Physical Chemistry of Solid Surfaces.

10.1021/jp035433d CCC: $27.50
Published on Web 12/20/2003

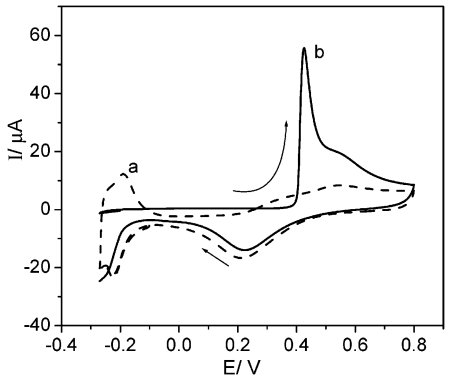

Figure 1. Cyclic voltammograms of a Rh electrode in 0.1 M H_2SO_4 without (a, dashed line) and with (b, solid line) CO. CO is bubbled into the solution for ca. 15 min at −0.2 V.

platinum ring served as the counter electrode. The reference electrode was a saturated calomel electrode (SCE), thus all the potentials in this paper were quoted versus SCE. All the chemicals used are of analytical reagents and the solutions were prepared using Milli-Q water.

The applied currents or potentials during the roughening and Raman measurements were controlled by a PAR 173 potentiostat (EG&G). Square-wave function was delivered by a GFG-8016G function generator (Good Will Instrument Co. Ltd.). Cyclic voltammograms (CV) were recorded with a CHI631A electrochemical workstation (CH instruments, Inc.).

The Raman measurements were performed on a confocal microprobe Raman system (LabRam I, Dilor). The laser excitation line was 632.8 nm from an internal He−Ne laser and the laser power on the sample was about 3 mW. A long working distance (8 mm) microscope objective having a 50× magnification and a numerical aperture of 0.55 was used.

Results and Discussion

Acidic Solutions. Since CO has been considered as one of the main poisoning intermediates produced from the dissociation of C_1 molecules during their electrooxidation, we performed the electrochemical and SERS study on the CO adsorption and its electrooxidation on the roughened Rh substrate in the acidic solution.

Figure 1 shows CVs of the Rh electrode in 0.1 M H_2SO_4 solution without and with CO. To ensure a saturated adsorption of CO, the CO gas was purged into the solution with the potential of the Rh electrode controlled at −0.2 V for 15 min. Compared with curve a in Figure 1, one can clearly see from curve b a strong suppression of hydrogen adsorption by the adsorbed CO. At potentials more positive than 0.4 V, an anodic peak appears corresponding to the electrooxidation of the adsorbed CO according to previous electrochemical and IR studies. By comparing the charge of the anodic peak in b to that in the hydrogen adsorption or desorption region in curve a of Figure 1, the coverage of CO (θ_{CO}) is calculated to be ca. 65%, which indicates the adsorption of CO on the Rh surface approaches the saturated adsorption.

On the basis of the electrochemical result, a SERS study of CO adsorption on Rh was performed with special care taken for the characteristic potentials. The SER spectra of adsorbed CO on the roughened Rh electrode in the 0.1 M H_2SO_4 solution are shown in Figure 2a. At potentials more negative than 0.4 V, where no discernible electrooxidation of CO can be observed, two bands in the high-frequency region related to the a-top and bridge-bound CO located at 2021 and 1887 cm^{-1}, respectively, can be clearly seen. Both species show a strong potential dependence. Their ν_{CO} frequencies blue-shift with increasing potential, see Figure 2b. Since there is no observable Faradaic current in this potential region, we assign the frequency shifts to the electrochemical Stark effect, i.e., the influence of the interfacial electric field and the back-donation of the substrate.[45−48] The change of the frequency with the electrode potential (also known as the Stark tuning rate) of ν_{CO} of the a-top CO is about 28 cm^{-1}/V. Meanwhile, in the lower-frequency region (300−700 cm^{-1}), one broad feature located at ca. 452 cm^{-1} can also be observed, which can be assigned mainly to ν_{RhC} of a-top CO according to refs 49 and 50. In our previous work on CO/Pt, although the CO band intensity of a-top CO is much stronger than that of the bridge-bound CO on the Pt surface,[15] the Pt−C(O)−Pt still gives a relatively stronger signal in the lower-frequency region. In the case of Rh, there is a comparable ν_{CO} signal for the a-top and bridge-bound CO; it is reasonable to assume that the broad feature located at ca. 452 cm^{-1} contains a considerable contribution of ν_{RhC} of the bridge-bound CO. This is further corroborated by the asymmetry of the 452 cm^{-1} band. At potentials more positive than 0.4 V, where the

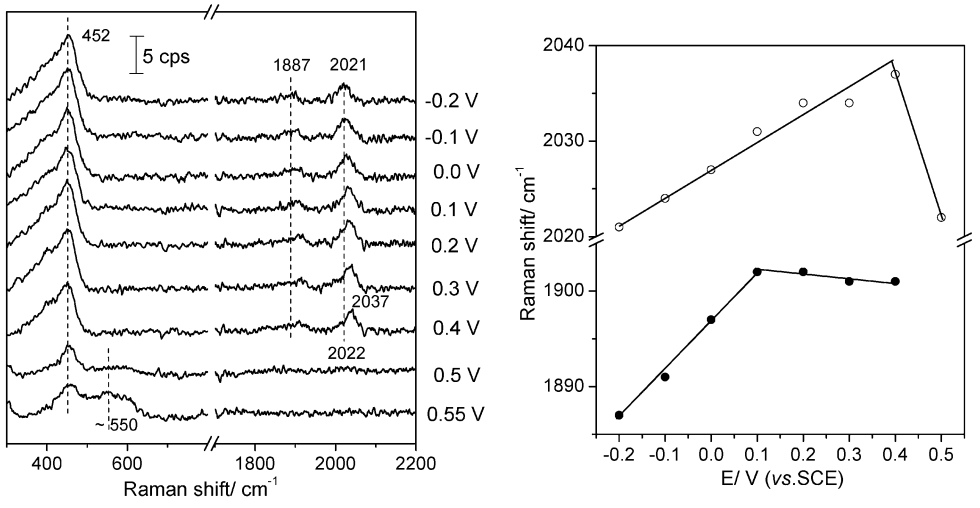

Figure 2. (a) Surface Raman spectra of a Rh electrode in 0.1 M H_2SO_4, after CO is bubbled to the solution at −0.2 V for 15 min. (b) A plot of frequencies of ν_{CO} of linear adsorbed CO (open circles) and the bridge-bond CO (closed circles) on Rh extracted from (a) with the electrode potential.

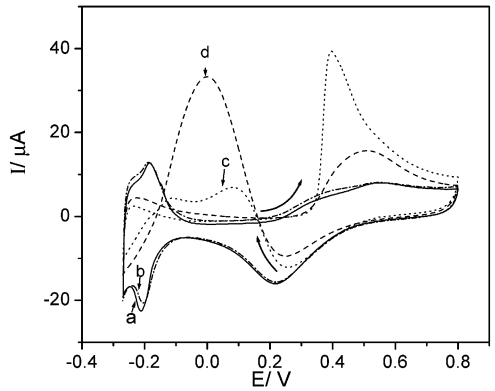

Figure 3. Cyclic voltammograms of a Rh electrode in 0.1 M H_2SO_4 (a, solid line) and in 0.1 M H_2SO_4 + 0.1 M CH_3OH (b, dash−dotted line), 0.1 M H_2SO_4 + 0.1 M HCHO (c, dotted line), and 0.1 M H_2SO_4 + 0.1 M HCOOH (d, dashed line).

electrooxidation of the adsorbed CO occurs, there remains only a very weak band at ca. 2022 cm^{-1}, while the 452 cm^{-1} band decreases only to about half of its maximum intensity. This is accompanied by the appearance of a new broad band located at ca. 550 cm^{-1}, which is attributable to the oxides at the Rh surface. This band grows rapidly when the potential is further positively moved. Although there is almost no discernible feature of ν_{CO} in the high-frequency region, there are still weak Raman features at ca. 452 cm^{-1}, indicating the remains of minor CO on the surface in the oxidation potential region. The detection of ν_{RhC} but no ν_{CO} signal in this potential region may be due to the following reasons: (1) ν_{RhC} has larger Raman scattering cross section compared to that of ν_{CO}. (2) During the oxidation process, the CO molecule changes its orientation significantly, e.g., from a perpendicular to a tilted or even flat one relative to the surface, while the Rh−C bond is only slightly tilted. This facilitates a combination and reaction with other adsorbed O atoms being present nearby at oxidation potentials; there is, therefore, less intensity change for the Rh−C band. One should note that using Raman spectroscopy one can easily obtain the vibrational information in the low-frequency region (<800 cm^{-1}), which is very difficult to achieve and still a challenge with IR spectroscopy.

With the basic knowledge of the CO adsorption, it is worthwhile performing the SERS study on the electrochemical dissociation and oxidation of C_1 organic molecules such as CH_3OH, HCHO, and HCOOH on the Rh electrode. For the sake of better comparison, 0.1 M H_2SO_4 was still used as the supporting electrolyte. The CVs for these species were given in Figure 3. As can be seen from curve a and b, there is only a slight difference between the CVs of the Rh electrode in the solution without and with CH_3OH because of the physisorption of CH_3OH on the electrode. However, the CVs of the Rh electrode in the solution containing 0.1 M HCHO and 0.1 M HCOOH show great difference, see curves c and d in Figure 3. Both of them present typical loops for the poisoning surface species. During the first positive scan starting from the negative side, the CV features are similar to that of the saturatedly adsorbed CO with lower oxidation currents and more negative potentials where the electrooxidation commences. The oxidation current of HCOOH is the lowest. However, during the following negative scan, anodic peaks appear at potentials immediately after the reduction of Rh surface oxides (with peak potential at 0.25 V). The anodic peaks are due to the electrooxidation of HCHO/HCOOH occurring immediately on the freshly reduced Rh surface without the poisoning of CO species. A higher anodic current in the negative scan for HCOOH than that for HCHO indicates that Rh is a better catalyst for the oxidation of HCOOH. Thus, we assign the anodic peaks observed in the first positive scan to the electrooxidation of the CO produced by the spontaneous dissociation of HCHO and HCOOH on the electrode surface. This can also be confirmed by the SER spectroscopic studies.

SERS studies were also performed for CH_3OH, HCHO, and HCOOH in 0.1 M H_2SO_4 solution. In agreement with our electrochemical investigation, besides the detection of vibrations related to H_2O, H_2SO_4, and CH_3OH in the solution, we did not detect any signal from the dissociated or oxidized species in the methanol solution. It indicates that Rh has no detectable activity to the electrochemical oxidation /dissociation of methanol in acidic media, which is different from the case of Pt.[15] The main reason may lie in the relatively weak interaction of Rh with hydrogen and stronger interaction with O and CO.[25] Figure 4a shows the SER spectra from the Rh electrode in the 0.1 M HCHO + 0.1 M H_2SO_4 solution. The spectra are also similar to that of saturatedly adsorbed CO, with slightly lower intensities, from which one may conclude that the adsorbed CO may be one of the poisons produced from the dissociation of HCHO. The differences lie in the following. First, the frequency of ν_{CO} of the a-top CO produced from the dissociation of HCHO is lower than that of CO adsorbed directly from CO-saturated solution. Similar result was observed for the bridge-bound CO,

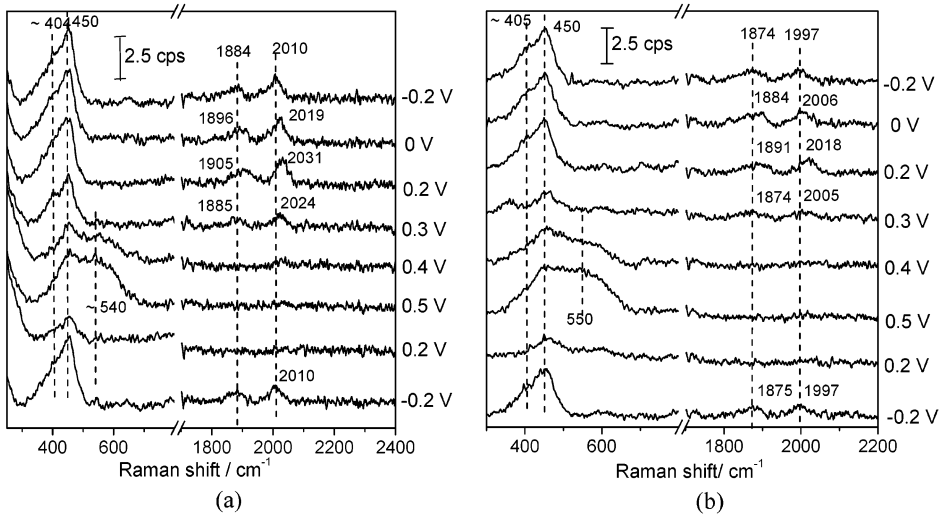

Figure 4. SER spectra of a Rh electrode in (a) 0.1 M H_2SO_4 + 0.1 M HCHO and (b) 0.1 M H_2SO_4 + 0.1 M HCOOH.

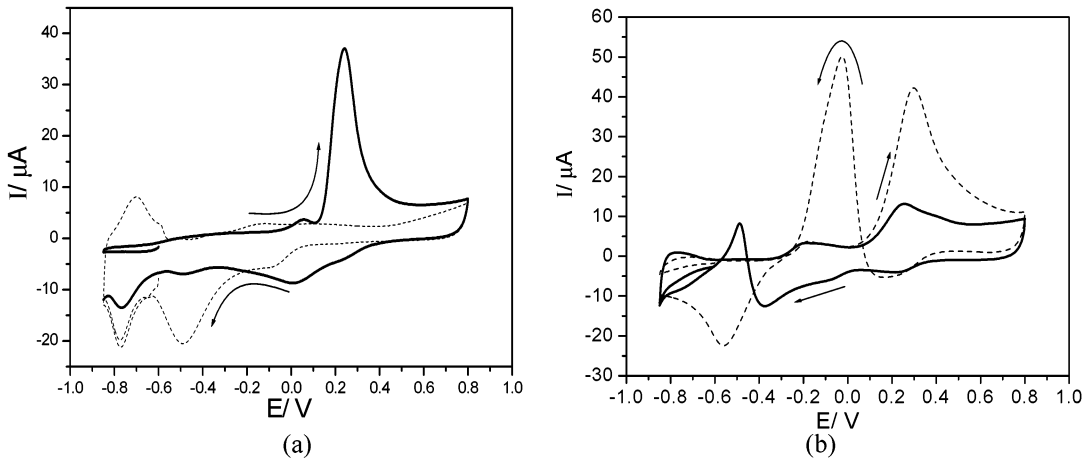

Figure 5. Cyclic voltammograms of a Rh electrode in 0.1 M Na_2SO_4 (dashed line in (a)) and after CO bubbling of the solution for 15 min (solid line in (a)), CH_3OH added into the solution to form 0.1 M Na_2SO_4 + 0.1 M CH_3OH (solid line in (b)), and HCHO added to the solution to form 0.1 M Na_2SO_4 + 0.1 M HCHO at −0.6 V (dashed line in (b)).

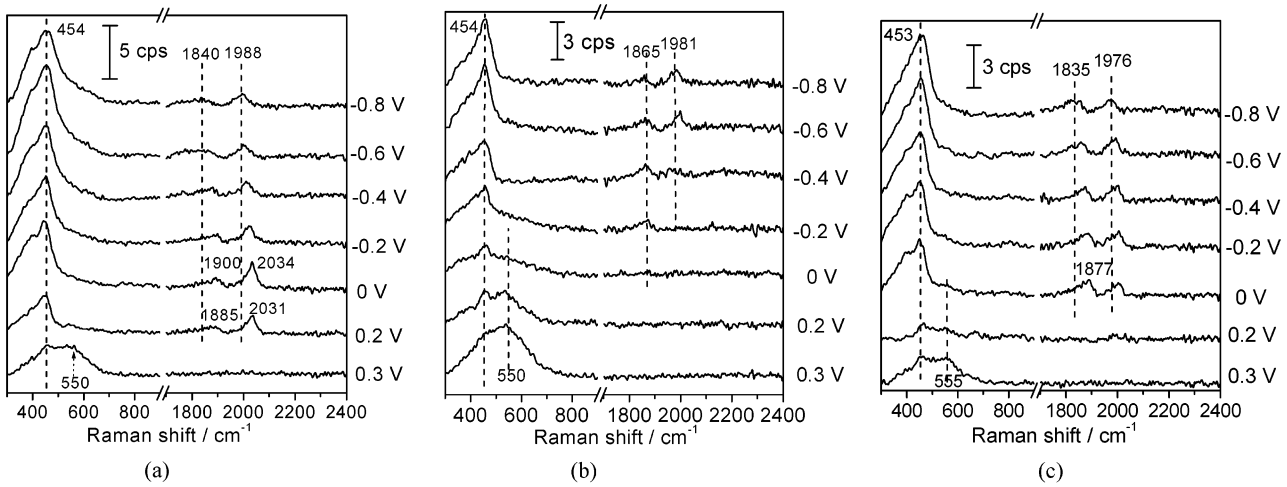

Figure 6. Surface Raman spectra of a Rh electrode in 0.1 M Na_2SO_4, with (a) CO bubbled to the solution for 15 min, (b) CH_3OH added into the solution to form 0.1 M Na_2SO_4 + 0.1 M CH_3OH, and (c) HCHO added into the solution to form 0.1 M Na_2SO_4 + 0.1 M HCHO at −0.6 V.

although not so obviously. Second, the intensity ratio for the Raman bands of the a-top CO to that of the bridge-bound CO is lower in the HCHO system compared to the CO system. The decrease in the intensity of ν_{RhC} and the appearance of the ν_{RhO} feature can also be observed at a more negative potential than that in the CO-saturated solution. At 0.3 V and more positive potentials where the electrooxidation of adsorbed CO occurs, the intensity of ν_{CO} decreases rapidly, accompanied by a decrease in the frequency. Furthermore, from the lower frequency of the ν_{CO} band in the case of HCHO one can conclude that the coverage of the adsorbed CO in the HCHO system is lower than the CO case, because a lower coverage will lead to a weaker dipole−dipole coupling among the adsorbed CO molecules, resulting in a lower vibrational frequency of CO. A lower coverage on one hand leads to a lower oxidation current and more negative oxidation potential, as can be seen from Figure 1 and Figure 3, and on the other hand may indicate that the dissociation of HCHO needs an additional site to accommodate H. After the oxidation of CO at 0.5 V and the return of the potential to 0.2 V, no signal in the higher-frequency region from CO can be observed, whereas in the lower-frequency region we observe a dramatic decrease in the band intensity of Rh oxide and a relatively lower intensity of the Rh−C band. However, the Raman feature of CO recovers almost totally when the potential is moved further negatively to −0.2 V.

A similar phenomenon occurs in the HCOOH case, see Figure 4b. However, one can find further lower frequencies of the CO stretch vibration for both the a-top and bridge-bound species. Moreover, the intensity ratio of the ν_{CO} bands of bridge-bound CO to that of the a-top CO is even large, indicating that the θ_{CO} in the HCOOH system is lower than that in the HCHO system, as supported by a lower oxidation current for CO in curve d in Figure 3. A possible reason may be that the dissociation of HCOOH needs more surface sites than HCHO, leading to a slightly lower coverage of the CO produced from dissociation.

Neutral and Alkaline Solutions. In the acidic solutions we found no discernible electrochemical activity of methanol on the Rh electrode. However, by considering a relatively strong interaction of Rh with OH^- and with the help of adsorbed OH^- on the surface, CH_3OH may dissociate and be further oxidized on the Rh surface in neutral and alkaline solutions. According to ref 5, the complete dissociation of adsorbed CH_3OH involves the generation of four protons, i.e.,

$$CH_3OH_{sol} \rightarrow CH_3OH_{ad} \rightarrow CO_{ad} + 4H^+ + 4e^-$$

Therefore, a higher OH^- concentration, i.e., a lower H^+ concentration, will force the reaction to occur in the right direction. For HCHO or HCOOH, the addition of OH^- may further improve their oxidation efficiency. Hence, one expects a dif-

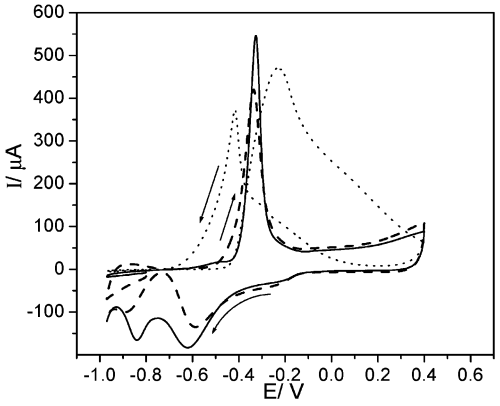

Figure 7. Cyclic voltammograms of a Rh electrode in 0.1 M NaOH with saturated CO (solid line) and 0.1 M CH_3OH (dashed line) and 0.1 M HCHO (dotted line) at the dosing potential of −0.8 V. Note that the current for the former two curves has been multiplied by a factor of 8.

ferent electrochemical behavior for the C_1 molecules in neutral and alkaline systems compared to that of the acidic system.

Figure 5 shows the CVs of the Rh electrode in the neutral Na_2SO_4 solution with saturated CO, and 0.1 M CH_3OH and HCHO at the dosing potential of −0.6 V. Since the behavior of HCOOH follows essentially the same trend as HCHO, we do not display the data here. The CV in the solution saturated with CO (Figure 5a, dashed line) only shows a slight difference in the shape compared to that of the acidic case. But a remarkable difference in CVs was observed for CH_3OH and HCHO. The CV in the CH_3OH solutions (Figure 5b, solid line) shows a small anodic peak commencing at ca. −0.3 V, and the major anodic peak commencing at ca. 0.0 V. On the basis of the knowledge of the acidic systems, this may be due to the electrooxidation of adsorbed CO. The commencing potential for the electrooxidation is, as in the case of the acidic system, more negative than that in the solution saturated with CO, see Figure 5a. In the negative scan a small anodic peak commences at ca. −0.4 V after the reduction of the oxides on the surface. This shows that Rh is not a good catalyst for CH_3OH oxidation compared with Pt.[25] The CV in HCHO solution (Figure 5b, dashed line) presents an anodic peak commencing at ca. 0 V in the positive scan for electrooxidation of CO, with a peak current relatively close to that in the acidic case. In the negative scan, the anodic peak commences at ca. 0.1 V when the surface oxides have not been totally reduced yet. The peak current is much higher than that in the acidic system, which shows that the electrocatalytic activity of Rh to the electrooxidation of HCHO is higher in the neutral solution.

Figure 6 shows SER spectra of the Rh electrode in the neutral Na_2SO_4 solution with saturated CO, and in 0.1 M CH_3OH and 0.1 M HCHO solution dipped at a potential of −0.6 V. In Figure 6a, one can see that the adsorbed CO from the saturated CO solution can exist stably at potentials more negative than 0.3 V. The SERS features of Figure 6b indicate that adsorbed CH_3OH is dissociated into CO on the electrode. But the CO bands decrease significantly in the potential range from −0.4 to −0.2 V, especially that of the a-top CO feature, and then disappear completely at 0 V. This may be correlated with the small anodic peak commencing at −0.2 V in the solid-line curve in Figure 5b. A higher ratio of the bridge-bound to a-top CO than that adsorbed from the saturated CO solution also indicates a lower coverage of CO generated from the dissociation of methanol. For the HCHO system (Figure 6c), the case is rather similar to that in the H_2SO_4 solution. The disappearance of the CO features and the appearance of the oxide feature occur at potentials more positive than 0 V. Compared to the acidic media, the frequencies of ν_{CO} are significantly red-shifted. But the frequencies of ν_{RhC} are slightly blue-shifted. The lower frequency of adsorbed CO still also indicates a low coverage of adsorbed CO compared with that adsorbed directly from solution saturated with CO.

A series of study will not be complete without the information from alkaline solutions. The CVs of the Rh electrode in 0.1 M NaOH solutions containing saturated CO, 0.1 M CH_3OH, and 0.1 M HCHO are shown in Figure 7, respectively. There is still no obvious difference for the saturated CO system in solutions of different pH except the slight change of the relative potential for oxide reduction. However, a great difference can be found for both the CH_3OH and HCHO systems, where the anodic currents in the positive scan increase significantly when the pH values increase, especially for the HCHO system. It may be due to a higher concentration of OH^-, leading to the increase in the dissociation rate of CH_3OH and HCHO. One can see the obvious adsorbed CO features from the SER spectra (shown in Figure 8) of the Rh electrode in NaOH solution containing CH_3OH and HCHO. It should be noted that, in the HCHO system, the signals from CO still exist at 0.1 V, however, in the saturated CO system and the CH_3OH system, CO has been already oxidized at −0.4 V. The main reason for this abnormal

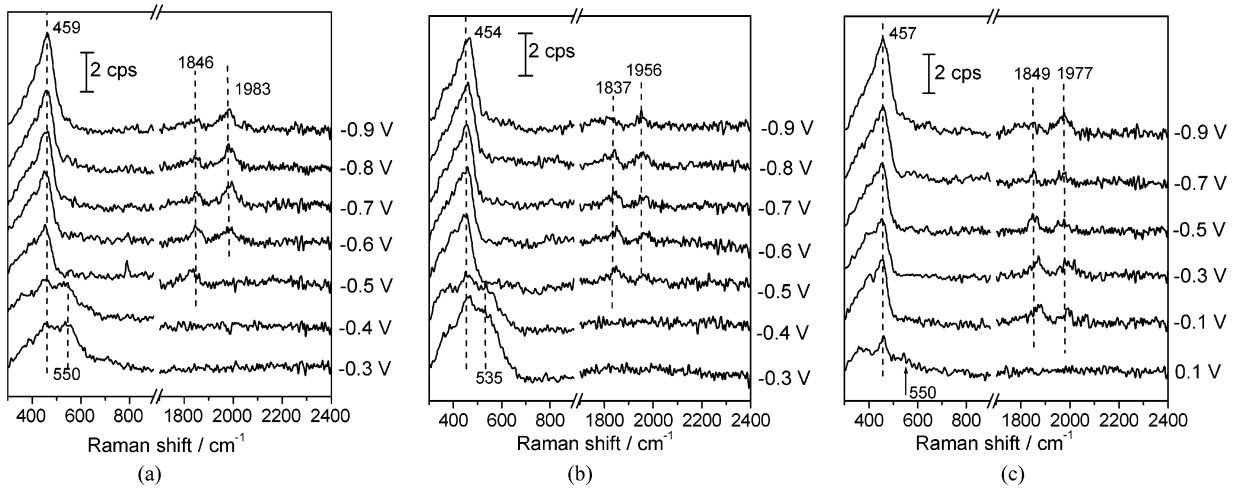

Figure 8. Surface Raman spectra of a Rh electrode in 0.1 M NaOH, with (a) CO bubbled to the solution for 15 min, (b) CH_3OH added into the solution to form 0.1 M NaOH + 0.1 M CH_3OH solution, and (c) HCHO added into the solution to form 0.1 M NaOH + 0.1 M HCHO at −0.8 V.

phenomenon may be due to the vigorous reaction of HCHO in the NaOH solution, which produces a large amount of H^+ and increases the local acidity around the electrode surface during the Raman measurement that need several minutes for collecting one Raman spectrum. Compared with the case of the neutral solutions, the frequencies of ν_{CO} are further red-shifted and the intensities further decrease probably due to the further lowering of the surface coverage in basic solution, and the interaction of neighboring adsorbed OH^-. The similar spectral features of the adsorbed CO and Rh oxides for the two systems show similar reaction mechanisms for CH_3OH and HCHO in solutions with different pH.

Conclusions

This study shows that SERS can be effectively used to study the electrocatalytic processes occurring on the appropriately roughened Rh electrode with a confocal microprobe Raman system. The very stable and reversible Rh substrate enables a comparison of the results from different electrolytes. Both electrochemical and SERS studies reveal that Rh has good activity in the electrooxidation of CO in acidic, neutral, and basic solutions. The oxidation potential for CO adsorbed from a CO-saturated solution shifts to a more negative value with increasing pH. However, the result for methanol is quite different and complicated either compared to CO and other C_1 molecules or to the case on Pt. No discernible electrooxidation current could be detected for CH_3OH in the acidic solution, probably due to the relatively weaker interaction of Rh with hydrogen and stronger interaction with O and CO compared to Pt in the acidic solution. However, with the assistance of the hydroxyl ions, CH_3OH can also be dissociated and oxidized in the neutral and slightly more efficiently in the alkaline solution. For the HCHO (also HCOOH)-containing electrolytes, the phenomena are relatively simple and similar. The oxidation of both species becomes easier with the increasing pH. The lower CO frequency in the HCHO (and HCOOH) case may indicate a slightly lower CO coverage, which may be due to the fact that the dissociation of HCHO needs more surface sites than CH_3OH. To account for the Rh−C and Rh−O vibrations in the low-frequency region during the oxidation process, where the Rh−C intensity does not decrease as much as the CO intensity does, we propose that the CO molecule may change its orientation significantly from perpendicular to a nearly horizontal one to facilitate the combination and reaction with nearby adsorbed O atoms. Our results show the unique advantage of SERS over other vibrational spectroscopies for the in-situ investigation of electrode interfaces, including the Rh surface. This type of study can easily be extended to binary metal systems, which is now still in progress in our lab; preliminary results have been published elsewhere.[51]

Acknowledgment. This work was funded by the National Natural Science Foundation of China (Contract Nos. 29903009, 20021002, 90206039). B.R. thanks Dr. Pettinger for careful editing of the English.

References and Notes

(1) Watanabe, M.; Motoo, S. *J. Electroanal. Chem.* **1975**, *60*, 267−273.
(2) Beden, B.; Bewick, A.; Kunimatsu, K.; Lamy, C. *J. Electroanal. Chem.* **1982**, *142*, 345−356.
(3) Parsons, R.; Van der Noot, T. *J. Electroanal. Chem.* **1988**, *257*, 9−45.
(4) Beden, B.; Lamy, C.; Leger, J.-M. In *Modern Aspects of Electrochemistry*; Bockris, J. O'M., Conway, B. E., White, R. E., Eds.; Plenum: New York, 1992; Vol. 22, p 97.
(5) Hamnett, A. In *Interfacial Electrochemistry*; Wieckowski, A., Ed.; Marcel Dekker: New York, 1999; p 843.
(6) Waszczuk, P.; Lu, G. Q.; Wieckowski, A.; Lu, C.; Rice, C.; Masel, R. I. *Electrochim. Acta* **2002**, *47*, 3637−3652.
(7) Bewick, A.; Pons, S. In *Advances in Infrared and Raman Spectroscopy*; Clark, R. J. H., Hester, R. E., Eds.; Wiley Hayden: Chichester, 1985; Vol. 12, p 1.
(8) Iwasita, T.; Nart, F. C. In *Surface Infrared and Raman Spectroscopy: Methods and Applications*; Suetaka, W., Ed.; Plenum: New York, 1995; p 126.
(9) Kunimatsu, K. *J. Electroanal. Chem.* **1986**, *213*, 149−157.
(10) Juanto, S.; Beden, B.; Hahn, F.; Leger, J. M.; Lamy, C. *J. Electroanal. Chem.* **1987**, *237*, 119−129.
(11) Iwasita, T.; Nart, F. C.; Lopez, N.; Vielstich, W. *Electrochim. Acta* **1992**, 37, 2361−2367.
(12) Vielstich, W.; Christensen, P. A.; Weeks, S. A.; Hamnett, A. *J. Electroanal. Chem.* **1988**, *242*, 327−333.
(13) Corrigan, D. S.; Weaver, M. J. *J. Electroanal. Chem.* **1988**, *241*, 143−162.
(14) Zhang, Y.; Weaver, M. J. *Langmuir* **1993**, *9*, 1397−1403.
(15) Ren, B.; Li, X. Q.; She, C. X.; Wu, D. Y.; Tian, Z. Q. *Electrochim. Acta* **2000**, *46*, 193−205.
(16) Weaver, M. J. *J. Raman Spectrosc.* **2002**, *33*, 309−317.
(17) Tadjeddine, A.; Peremans, A.; Guyotsionnest, P. *Surf. Sci.* **1995**, *335*, 210−220.
(18) Watanabe, N.; Iwatsu, K.; Yamakata, A.; Ohtani, T.; Kubota, J.; Kondo, J. N.; Wada, A.; Domen, K.; Hirose, C. *Surf. Sci*. **1996**, *357/358*, 651−655.
(19) Vidal, F.; Busson, B.; Six, C.; Pluchery, O.; Tadjeddine, A. *Surf. Sci.* **2002**, *502*, 485−489.
(20) Gao, P.; Lin, C. H.; Shannon, C.; Salaita, G. N.; White, J. H.; Chaffins, S. A.; Hubbard, A. T. *Langmuir* **1991**, *7*, 1515−1524.
(21) Wang, J. H.; Masel, R. I. *J. Am. Chem. Soc.* **1991**, *113*, 5850−5856.
(22) Zei, M. S.; Ertl, G. *Phys. Chem. Chem. Phys.* **2000**, *2*, 3855−3859.
(23) Iwasita, T.; Vielstich, W. *J. Electroanal. Chem.* **1986**, *201*, 403−408
(24) Pastor, E.; Schmidt, V. M.; Iwasita, T.; Arevalo, M. C.; Gonzalez, S.; Arvia, A. J. *Electrochim. Acta* **1993**, *38*, 1337−1344.
(25) de Souza, J. P. I.; Queiroz, S. L.; Bergamaski, K.; Gonzalez, E. R.; Nart, F. C. *J. Phys. Chem. B.* **2002**, *106*, 9825−9830.
(26) Day, J. B.; Vuissoz, P. A.; Oldfield, E.; Wieckowski, A.; Ansermet, J. P. *J. Am. Chem. Soc.* **1996**, *118*, 13046−13050.
(27) Moskovits, M. *Rev. Mod. Phys*. **1985**, 57, 783−826.
(28) Otto, A.; Mrozek, I.; Grabhorn, H.; Akemann, W. *J. Phys. Condens. Matter* **1992**, 4, 1143−1212.
(29) Campion, A.; Kambhampati, P. *Chem. Soc. Rev.* **1998**, *27*, 241−250.
(30) Pettinger, B. In *Adsorption at Electrode Surface*; Lipkowski, J. Ross, P. N., Eds.; VCH: New York, 1992; p 285.
(31) Birke, R. L.; Lombardi, J. R. In *Spectroelectrochemistry—Theory and Practice*; Gale, R. J. Ed.; Plenum: New York, 1988; p 263.
(32) Chan, H. Y. H.; Williams, C. T.; Weaver, M. J.; Takoudis, C. G. *J. Catal*. **1998**, *174*, 191−200.
(33) Williams, C. T.; Takoudis, C. G.; Weaver, M. J. *J. Phys. Chem. B* **1998**, *102*, 406−416.
(34) Tian, Z. Q.; Ren, B.; Wu, D. Y. *J. Phys. Chem. B* **2002**, *106*, 9463−9483.
(35) Leung, L.-W. H.; Weaver, M. J. *J. Am. Chem. Soc.* **1987**, *109*, 5113−5119.
(36) Zou, S. Z.; Williams, C. T.; Chen, E. K. H.; Weaver, M. *J. J. Am. Chem. Soc.* **1998**, *120*, 3811−3812
(37) Zou, S. Z.; Weaver, M. J. *Anal. Chem.* **1998**, *70*, 2387−2395.
(38) Zou, S. Z.; Williams, C. T.; Chen, E. K. H.; Weaver, M. J. *J. Phys. Chem. B* **1998**, 102, 9039−9049.
(39) Tian, Z. Q.; Ren, B.; Mao, B. W. *J. Phys. Chem. B* **1997**, *101*, 1338−1346.
(40) Tian, Z. Q.; Gao, J. S.; Li, X. Q.; Ren, B.; Huang, Q. J.; Cai, W. B.; Liu, F. M.; Mao, B. W. *J. Raman Spectrosc.* **1998**, *29*, 703−711.
(41) Huang, Q. J.; Li, X. Q.; Yao, J. L.; Ren, B.; Cai, W. B.; Gao, J. S.; Mao, B. W.; Tian, Z. Q. *Surf. Sci.* **1999**, *428*, 162−166.
(42) Ren, B.; Lin, X. F.; Jiang, Y. X.; Cao, P. G.; Xie, Y.; Huang, Q. J.; Tian, Z. Q. *Appl. Spectrosc.* **2003**, *57*, 419−427.
(43) Ren, B.; Lin, X. F.; Tian, Z. Q. *Chin. J. Electrochem*. **2001**, *7*, 55−58.
(44) Ren, B.; Lin, X. F.; Yan, J. W.; Mao, B. W.; Tian, Z. Q. *J. Phys. Chem. B* **2003**, *107*, 899−902.
(45) Korzeniewski, C.; Shirts, R. B.; Pons, S. *J. Phys. Chem.* **1985**, *89*, 2297−2298.
(46) Lambert, D. K. *Electrochim. Acta* **1996**, *41*, 623−630.
(47) Zou, S. Z.; Weaver, M. J. *J. Phys. Chem.* **1996**, *100*, 4237−4242.
(48) Wasileski, S. A.; Koper, M. T. M.; Weaver, M. J. *J. Am. Chem. Soc.* **2002**, *124*, 2796−2805.
(49) Gurney, B. A.; Richter, L. J.; Villarrubia, J. S.; Ho, W. *J. Chem. Phys.* **1987**, *87*, 6710−6721.
(50) Dubois, L. H.; Somorjai, G. A. *Surf. Sci.* **1980**, *91*, 514−532.
(51) She, C. X.; Xiang, J.; Ren, B.; Wang, X. C.; Tian, Z. Q. *J. Korean Electrochem. Soc.* **2002**, *5*, 221−225.